

Supplemental Information

Pathogen-Specific Treg Cells Expand Early during *Mycobacterium tuberculosis* Infection but Are Subsequently Eliminated in Response to Interleukin-12

Shahin Shafiani, Crystal Dinh, James M. Ertelt, Albanus O. Moguche, Imran Siddiqui, Kate S. Smigiel, Pawan Sharma, Daniel J. Campbell, Sing Sing Way, and Kevin B. Urdahl

Inventory of Supplemental Data

Figure S1, Detection of Mtb-specific Treg cells in the pLN of Mtb-infected mice. Related to Figure 1.

Figure S2, Direct ex-vivo intracellular IFN- γ staining by ESAT-6₄₋₁₇:I-A^b-binding CD4⁺ T cells at day 25 post-infection. Related to Figure 2.

Figure S3, Mtb-specific Treg cells are not selected on an alternative TCR α chain. Related to Figure 3.

Figure S4, Intranasal infection with *Listeria monocytogenes* induces minimal expansion of Treg cells specific to a native antigen. Related to Figure 4.

Figure S5, IL-2/anti-IL-2 complex does not rescue the Mtb-specific Treg cells.

Figure S6, Mtb-specific Treg cell contraction is driven by IL-12. Related to Figure 6.

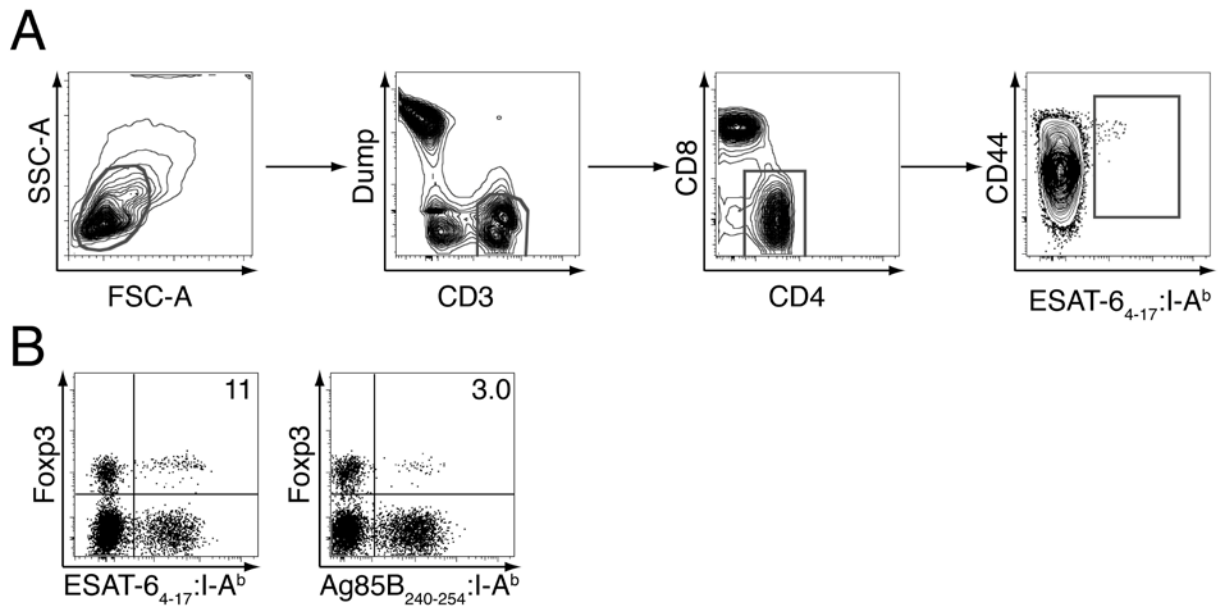


Figure S1 Detection of Mtb-specific Treg cells in the pLN of Mtb-infected mice. (A) Gating strategy used to demonstrate cells binding the ESAT-6₄₋₁₇-I-A^b tetramer and expression of activation marker CD44, 21 days post Mtb infection. (B) Treg cells in the pLN also recognize a second Mtb-epitope. Expression of Foxp3 and ESAT-6₄₋₁₇-I-A^b or Ag85B₂₄₀₋₂₅₄-I-A^b tetramer-binding by CD4-gated cells within pLN cells (day 21 post-infection) co-enriched for cells binding either tetramer. Numbers represent the percentage of tetramer-binding cells expressing Foxp3. See also Figure 1.

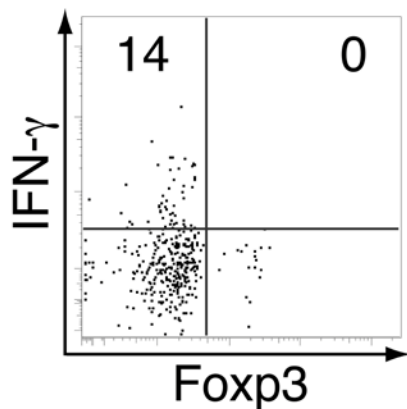


Figure S2 Direct ex-vivo intracellular IFN- γ staining by ESAT-6₄₋₁₇-I-A^b-binding CD4⁺ T cells at day 25 post-infection. Numbers represent the percentage of tetramer-binding Foxp3^{neg} or Foxp3⁺ cells producing IFN- γ . Representative data from two experiments performed at this timepoint are shown. See also Figure 2.

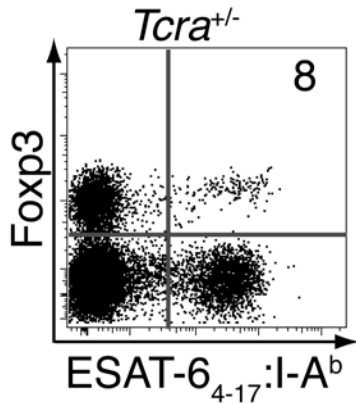


Figure S3 Mtb-specific Treg cells are not selected on an alternative TCR α chain. Expression of Fcγp3 and tetramer-binding by CD4-gated cells within tetramer enriched pLN cells of TCR $\alpha^{+/-}$ mice on day 21 post-infection. Number represents the percentage of tetramer-binding cells expressing Fcγp3. The experiment was performed three times and representative data are shown. See also Figure 3.

Figure S4 Intranasal infection with *Listeria monocytogenes* induces minimal expansion of Treg cells specific to a native antigen. Expression of Fcγp3 and LLO₁₉₀₋₂₀₁:I-A^b tetramer-binding by CD4-gated cells within pLN cells on day 8 post intranasal infection with 1×10^8 ActA-deficient *Listeria monocytogenes* after enrichment for tetramer-binding cells. Numbers represent the percentage of tetramer-binding cells expressing Fcγp3. See also Figure 4.

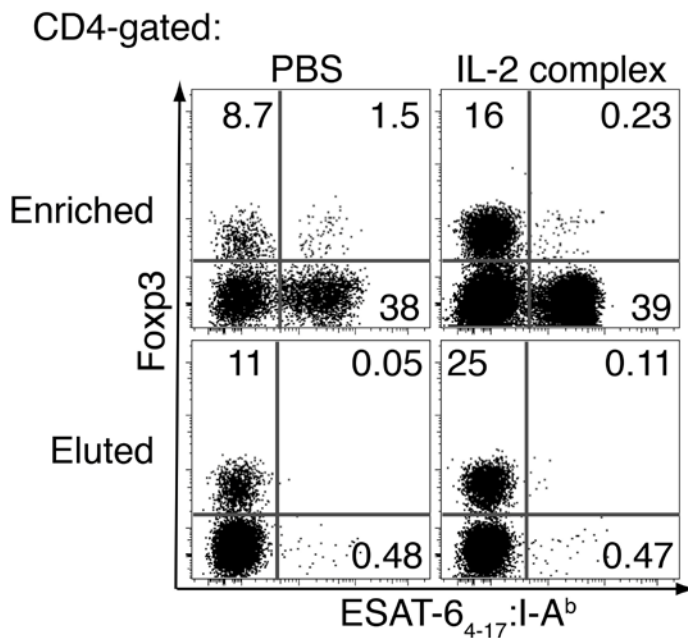
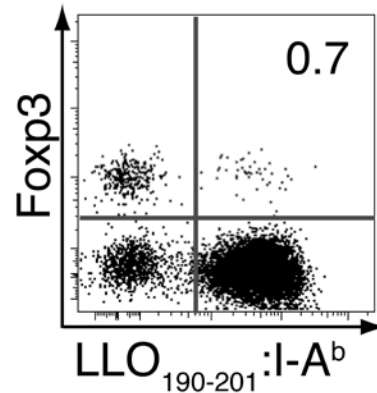


Figure S5 IL-2/anti-IL-2 complex does not rescue the Mtb-specific Treg cells. Gated on CD4⁺ T cells, tetramer binding and Fcγp3 expression is shown in the enriched and eluted fraction of the pLNs of mice on day 25 post Mtb infection. The mice received daily doses of either IL-2/anti-IL-2 complex or PBS for 5 consecutive days prior to being harvested.

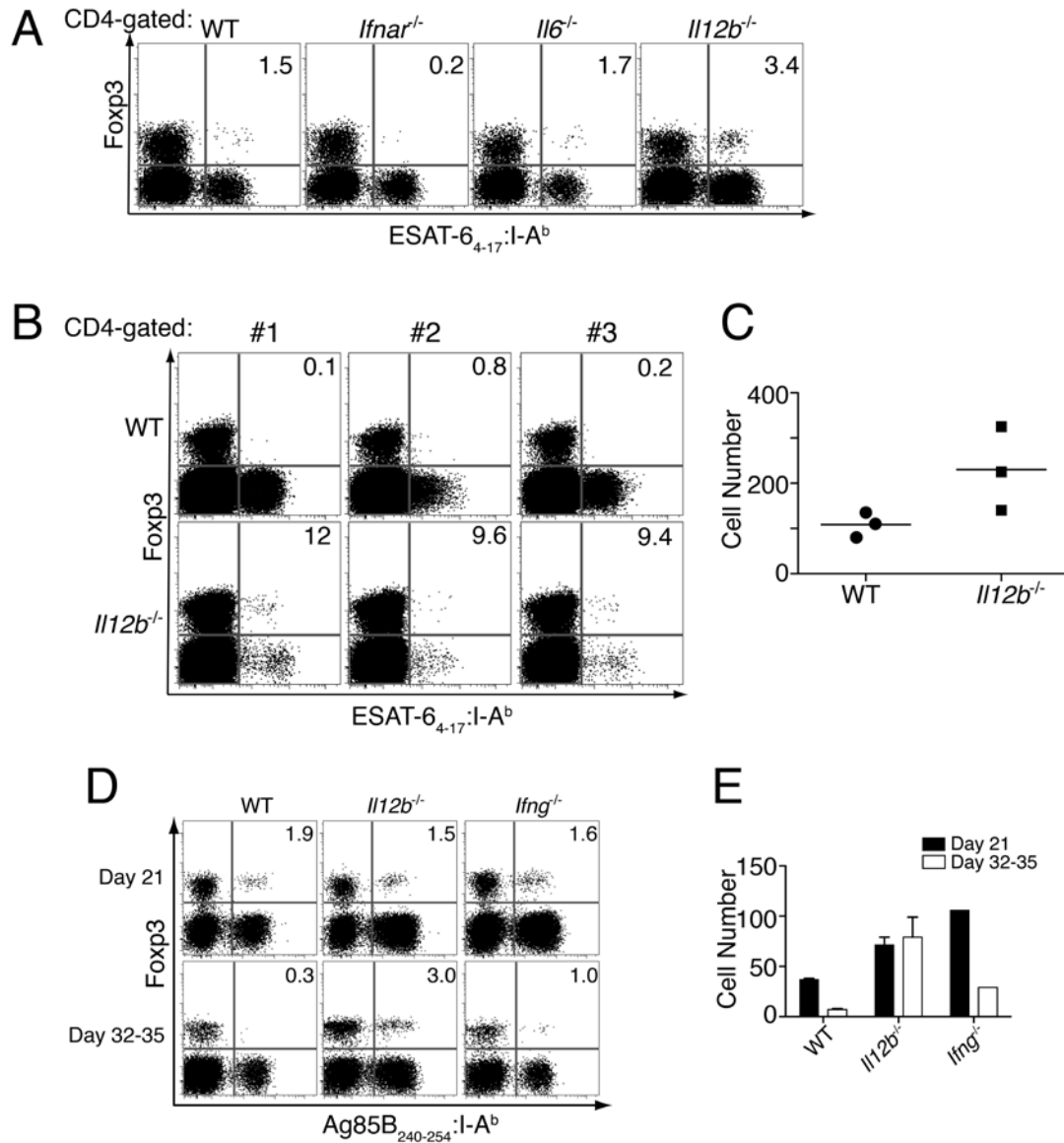


Figure S6 Mtb-specific Treg cell contraction is driven by IL-12. (A) FACS plots show CD4-gated cells stained for tetramer and Foxp3 from the enriched pLNs of Mtb-infected wild type B6, *Ifnar*^{-/-}, *Il6*^{-/-}, and *Il12b*^{-/-} mice on day 26 post-infection. Numbers in the quadrants represent the percentage of Foxp3⁺ cells within the tetramer-binding population. Experiment was performed once for *Ifnar*^{-/-} and *Il6*^{-/-} mice, three times for *Il12b*^{-/-} mice and 5 times for WT B6 mice. (B) FACS plots show CD4-gated cells stained for tetramer and Foxp3 from Mtb-infected control wild type B6 and *Il12b*^{-/-} mice on day 26 post-infection. Numbers in the quadrants represent the percentage of Foxp3⁺ cells within the tetramer-binding population. Data from three individual mice of each group are shown. (C) Graph represents absolute number of tetramer binding Treg cells in the lungs of both groups. Each

solid square and circle represents an individual mouse; bars indicate the mean of each group. (D) FACS plots represent column-enriched pLNs from Mtb-infected control wild type (WT) B6 mice, and mice deficient in IL-12p40 and IFN γ , analyzed for binding to a tetramer with specificity for a different Mtb epitope (Ag85B₂₄₀₋₂₅₄:I-A^b) and Foxp3 expression. Mice were harvested at day 21 and 35 post-infection with the exception of IFN- γ -deficient mice which were analyzed at day 32 because they had lost 20% of their body weight and appeared near death. Numbers in the quadrants represent the percentage of Foxp3⁺ cells within the tetramer-binding population. Experiments were performed four times for the WT and IL-12p40-deficient mice and once for the IFN- γ -deficient mice. Representative plots are shown. (E) Bar graphs represent absolute number of tetramer binding Treg cells at the two timepoints in the mentioned groups. Mean \pm SEM is shown for the WT and *Il12b*^{-/-} groups. See also Figure 6.